Received 4 August 2019; revised 15 September 2019 and 15 October 2019; accepted 16 October 2019. Date of publication 21 October 2019; date of current version 30 October 2019. The review of this article was arranged by Editor S. Vaziri.

Digital Object Identifier 10.1109/JEDS.2019.2948375

Graphene Nano Sheet Fabrication Using Light

HONGLIANG SUN [1,2,3] **(Member, IEEE)**

1 State Key Laboratory for Manufacturing Systems Engineering, School of Mechanical Engineering, Xi'an Jiaotong University, Xi'an 710049, China
2 Yunnan Key Laboratory for Micro/Nano Materials and Technology, Yunnan University, Kunming 650091, China
3 School of Mechanical and Electrical Engineering, Yunnan Open University, Kunming 650223, China

CORRESPONDING AUTHOR: H. SUN (e-mail: hlsun@aliyun.com)

This work was supported in part by the National Natural Science Foundation of China under Grant U1505244, in part by the State Key Laboratory of Manufacturing Systems Engineering under Grant SKLMS2018007, and in part by the Open Project of Yunnan Key Laboratory of Micro/Nano Materials and Technology under Grant KF2016005.

ABSTRACT The photochemical-reduction methods exhibit many interesting applications in metal and metal oxide nanoparticles with promising properties such as easy-to-handle, easy-to-inkjet and cost-effective. Using the soluble graphene oxide (GO) as a precursor, graphene production can be achieved via photochemical reduction, paving the way for manufacturing graphene products in controllable microscopic patterns. In this work, I used a photochemical method to obtain reduced graphene oxide (rGO), assisted by strong reducing α-aminoalkyl (α-A*) radicals generated by photoinitiator Irgacure-907. The extent of oxygen reduction can be continually controlled by manipulating light dosage and characterized by quantitative measurements of structure, morphology, chemical composition and electrical conductivity. The high quality of obtained rGO makes this photochemical-reduction based technology ideal for inkjet printing microstructures of graphene, thus achieving desirable conductivity, other physical and chemical properties associated.

INDEX TERMS Photochemical reduction, graphene nano sheet, photoinitiator, light.

I. INTRODUCTION

Graphene is a one-atom-thick two-dimensional (2-D) sheet consisting of sp^2-hybridized carbon atoms arranged in a honeycomb-like lattice. Graphene possesses a super-large surface area (2630 m^2g^{-1} for the theoretical value of fully exfoliated pristine graphene) [1], high thermal conductivity [2], strong mechanical strength [3], and superior electric conductivity [4]. The material properties of graphene have drawn broad attention in recent years, and it has been broadly applied in electronic devices [5], solar energy storage and conversion [6], [7], sensors [8], catalysis [9], biomedical materials [10], [11], and 3D printing materials [12]–[15]. Currently, graphene is often obtained through three pathways, micromechanical exfoliation [16], chemical vapor deposition (CVD) [17] and chemical reduction of GO [18]. The most widely used method is chemical reduction because it allows for mass production [19]. The chemical reduction relies on highly active but hazardous reductants, like hydrazine and hydrazine derivatives [20] or sodium borohydride [21] which may produce undesirable by-products. Although the chemical reduction is effective and is easily realized in the laboratory, industrial manufacturers would not be satisfied with the toxic reduction processes applied in chemical reduction. Inkjet printing provided an alternative way of making high-quality graphene and corresponding nanomaterials with minimal toxic reagents and by-products.

Graphene, like many other carbon-based materials, repels water, a property often known as being hydrophobic. Since graphene can be hardly dissolved in most solvents, auxiliary solvent like dimethylformamide (DMF) and N-methyl pyrrolidone (NMP) is often added to improve the solubility of graphene suspension when employed in inkjet printing [22]. On the contrary, graphene oxides (GOs) have better solubility owning to the oxygen-containing groups (OCGs) and have been used as effective source material to produce graphene through reduction. The disadvantage of OCGs is that they make GO insulating and restrict its applications in fabricating electronic devices. To take both advantages of GO and rGO, some researchers put forward a method that used GO ink as a 3D printing precursor and then applied reduction treatment to get the designed structure of conductive rGO [23], [24]. Though this is a viable strategy in principle and several approaches

have been established around this idea, there are several drawbacks. Liquid exfoliation requires an extended period of time or high intensity of ultrasonic vibration for the rGO suspension, which is known to reduce the size of exfoliated graphene and could decrease the electrical conductivity. High-temperature thermal reduction treatment is only limited heat resistant substrates. Hydrazine vapor reduction has to employ toxic vapor, making it restricted to be used in an open environment. A user-friendly and widely applicable GO reduction method is in great desire.

Recently, GO reduction based on light irradiation was demonstrated. The photochemical reduction method employed photosensitizers which released free radicals under light exposure. The free radicals are strong reducing agents and have shown great promise in synthesizing tunable and green products of metal (Au, Ag, Pt), metal oxide (Co_3O_4, SnO_2, Fe_2O_3), or biomaterials to bionics. The photochemical efficiency mainly depends on the photon energy (electromagnetic frequency) and less prone to the total illumination power. Compared with chemical methods, the photochemical reduction offers some unique advantages including spatial and temporal control, economical effectiveness, and green synthetic routes. These properties make it feasible to develop a sustainable and scale-up synthesis of graphene or *in situ* preparation of graphene-metal/metal oxide nanocomposites, which results in extensive scientific reports [25]–[28]. It is worth noting that if photocatalyst was not used, it required very long irradiation time even up to 48 hours [27]. In 2015, Tu *et al.* used a scanning probe to measure the electrical properties of vacuum-ultraviolet (VUV) rGO with an irradiation time reduced to 64 mins [25]. In 2017, Mangadlao et.al used tetrahydrofuran as solution and I-2959 as photoinitiator, and produced rGO-nanoparticle hybrid in 30min [26]. In 2019, Karin *et al.* added argon gas to keep the aqueous solution free of reaction during UV radiation with an irradiation time of 3 hours [28]. However, requirements of long operating time, vacuum environment and inert gas protection are only suitable for laboratory conditions but practical production.

In this work, 2-methyl-1-[4-(methylthio) phenyl]-2-morpholinopropanone-1 (Irgacure-907) was used as a photoinitiator. It has been approved that I-907 has more advantages of reducing transition metals than I-2959 since I-907 has stronger reduction ability of ketyl radicals [28]. The photochemical reaction belongs to the photochemical Norrish Type-I reaction, characterized by employing α-cleavage to form strong reducing radicals. As illustrated in Fig. 1, upon photoexcitation by UV light (Panasonic Aicure UP50), the Irgacure-907 generates α-aminoalkyl radicals (α-A*),which presents strong chemical reduction and donates electrons to the oxygen-containing groups in the GO with similar reaction process explained by Wee *et al.* [29]. Various complementary methods, which included X-ray photoelectron spectroscopy (XPS), atomic force microscopy (AFM), Fourier transform infrared spectroscopy (FTIR), Raman spectroscopy and electron

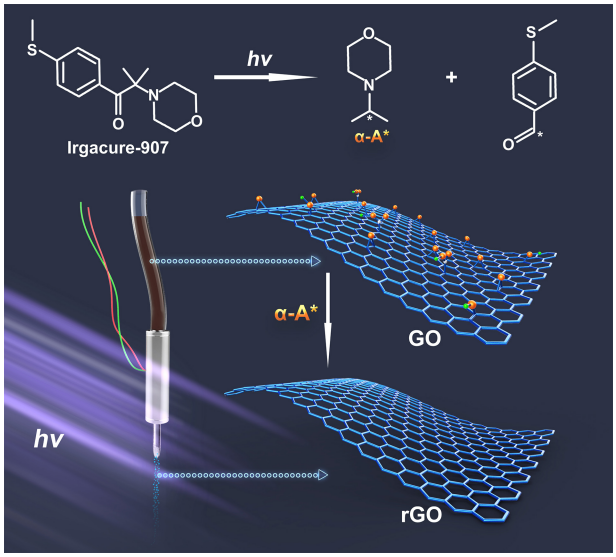

FIGURE 1. **The mechanism for generation of α-A* free radicals by photosensitizer Irgacure-907 and photochemical reduction of GO.**

microscopy, electrical conductivity measurement was used to characterize the morphological properties, chemical composition and electrical conductivity of rGO.

II. MATERIAL AND METHOD

1. *Synthesis of Graphene Oxide (GO):* The GO sheets were prepared using a modified Hummers method from graphite flakes [30]. Graphite powder (5.0 g) was put into a solution of concentrated H_2SO_4 (115.0 mL) and $NaNO_3$ (2.5 g). $KMnO_4$ (15.0 g) was slowly added to the reaction mixture under stirring and the temperature of the mixture was kept to be below 2 °C by cooling. Then, the mixture was stirred at 35 °C for 2 h, and then diluted with DI water (250.0 mL). The addition of water was carried out in an ice bath to keep the temperature below 50 °C. After adding all of the 250.0 mL DI water, the mixture was stirred for 2 h, and then additional 700.0 mL DI water was added. Shortly after the dilution with 700 mL DI water, 5 mL of 30 % H_2O_2 was added to the mixture, and the color of mixture changed into brilliant yellow along with bubbling. The mixture was filtered and washed with 1:10 HCl aqueous solution (1.0 L) to remove metal ions followed by DI water to remove the acid. The resulting solid was dried in a vacuum oven (DZF-6050, Shanghai Boxun Ind. & Comm. Co., Ltd., China) and diluted to make a graphite oxide (1.0 mg mL^{-1}). The achieved graphite oxide was sonicated under the ambient condition for 30 min (JY92-IIDN, Ningbo Scientz Biotechnology Co., Ltd., China). Graphene oxide (GO) dispersion was carried out after sonicated and was stable for a long time.

2. *Photochemical Reduction of GO:* To prepare for the typical photochemical reduction of GO precursor, 3.75 mL of dry acetonitrile was slowly added to 5.0 mL GO aqueous dispersion (1.0 mg mL^{-1}). After mixing with a magnetic stirrer bar for 10 minutes, 1.25 mL Irgacure-907 (100 mmol L^{-1})

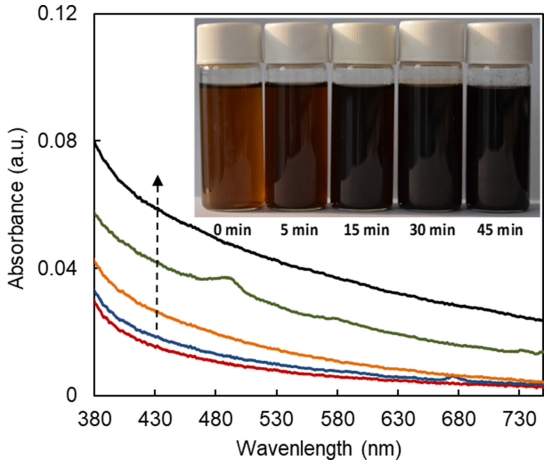

FIGURE 2. UV-VIS light extinction spectra of the GO solution in the presence of Irgacure-907 with respect to various UVA-irradiation periods. The inserted figure shows the photographs of the color change of the dispersions.

was uniformly dispersed in the mixed solution in a quartz tube and then irradiated with UV light for pre-designed periods varying in the range of 0-45 minutes. The induced photochemical reduction was further evidenced by measuring light extinction in the full visible wavelength range.

The color of GO solution gradually changed from light brown to dark brown and finally black, with respect to increased UV-irradiation time (Fig. 2). The change of color suggested that the photochemical reduction of GO took place with the release of reducing free radicals (α-A*) from the photochemical process. The temporal restoration of the aromatic π-bond network within the carbon structure is responsible for the insolubility of rGO [31]. Following the photochemical reduction, the rGO solution acquired was centrifugated and washed using dry acetonitrile for three times to remove the remaining Irgacure-907. All chemicals used in the experiment were in analytical-grade. Irgacure-907 was obtained from Shanghai Hound-Chase Fine Chemical Co. Ltd. China and the other reagents were purchased from Tianjin Benchmark Chemical Reagent Co. Ltd., China.

3. *Atomic Force Microscopy (AFM) Observation:* Atomic force microscopic (AFM) images were taken out using a Nanoscope Multimode SPM (Digital Instruments) with an AS-12 scanner operated in tapping mode in conjunction with a V-shaped tapping tip. The images were taken at a scan rate of 1.0 Hz. The AFM images were analyzed using NT-MDT Image Analysis software.

4. *X-ray Photoelectron Spectrometer (XPS) Analysis:* Determination of the chemical composition of the GO and rGO was made by using an X-ray photoelectron spectrometer (XPS; PH1-5700 ESCA system, U.S.) equipped with a hemispherical analyzer and an aluminum anode (monochromatic Al Kα 1486.6 eV) as source (at 12-14 kV and 10-20 mA). The system was operated under a retarding model with a binding energy of 20-980 eV. The peaks were calibrated with reference to C1s (284.6 eV).

5. *UV-vis, FT-IR, and Raman Spectroscopy:* Absorption was evaluated with extinction measurements using a UV-2550 UV-vis spectrometer (Shimazu, Japan) for the aqueous suspension of GO or rGO. The FT-IR spectra were obtained on a Fourier Transform Infrared spectrometer (Spectrum ONE B, PerkinElmer, U.S.). The dried GO or rGO were ground down into powder for FT-IR measurements. To study the defect formation, Raman spectra (Renishaw 2000 Confocal Raman Microprobe, U.K.) were recorded in the range of 1000-2000 cm^{-1} excited with an argon ion laser (514 nm).

6. *Electron Microscopy Imaging:* Transmission electron microscopy (TEM, F-30ST, Tecnai, FEI, U.S.) and scanning electron microscopy (SEM, Quanta 200FEG FEI, U.S.) imaging were performed to evaluate the sample quality. Prior to imaging, the GO and rGO samples were sonicated and suspended in ethanol solution. They were then drop-casting onto carbon-coated copper grids and then dried by evaporation at room temperature.

7. *Electrical Conductivity Measurements:* The powders samples were first compressed under the pressure of 12 MPa into round shape disks (d=13 mm) at room temperature by a commercial powder compressing machine (FW-4A, Tianjin TianGuang Optical Instruments Co., Ltd.). The electrical conductivity of the compressed samples was measured using the digital four-probe unit (ST2253, Suzhou Jingge Electronic Co., Ltd), counting disk thickness. For each sample type (GO, rGO, graphene), three samples were used with five conductivity measurements on each sample. The direction of lines of four touchpoints is evenly distributed as 0°, 72°, 144°, 216°, and 288°. The average results from all readings within the same group were used for assessing the level of electrical conductivity.

III. RESULTS AND DISCUSSION

Following the procedure of photochemical reduction, the resultant rGO solution was washed and dried for AFM imaging. For comparison, AFM was also performed on the single-layer GO sheet by exfoliation (Fig. 3a), which read approximate 1.2 nm in typical vertical thickness, consistent with the data reported in the literature [32]. After the photochemical reduction, the typical thickness of a single rGO sheet was reduced to 0.9 nm (Fig. 3b), significantly thinner than that of the GO sheet. From the 3D AFM images of mica-immobilized single-layer GO sheet and photochemically reduced GO (Fig. 4), it can be easily found that the thickness of photochemically reduced GO sheet was much less than the original sample. The decrease of rGO thickness observed in AFM further proved the removal of functional groups by strong reducing α-aminoalkyl radicals. Though the theoretical thickness of a single-layered graphene sheet is 0.34nm [32], rGO is often bigger in thickness (0.4-1.7nm) due to the presence of remaining oxygen-containing functional groups [33], [34]. The morphology of rGO after 45-min VA exposure was further characterized by scanning electron microscopy (Fig. 5a) and transmission electron

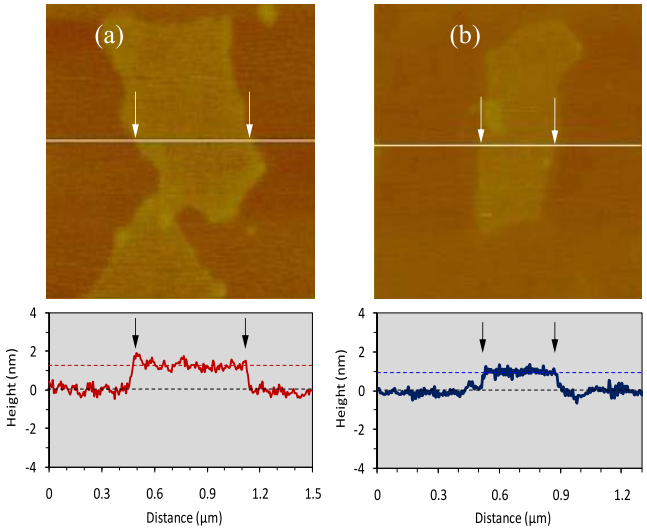

FIGURE 3. AFM images of mica-immobilized (a) single-layer GO sheet and (b) photochemically reduced GO (45-min UV exposure).

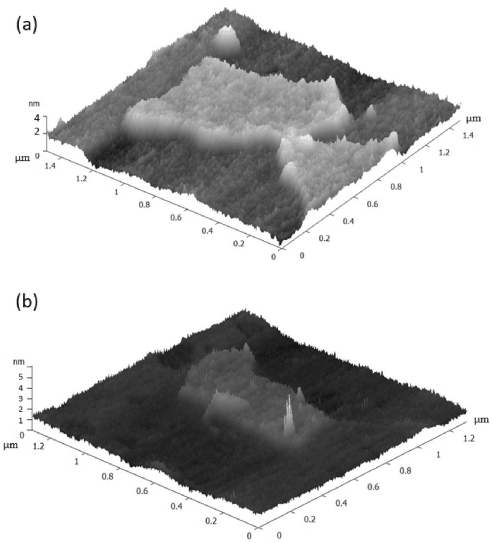

FIGURE 4. 3D AFM images of mica-immobilized (a) single-layer GO sheet and (b) photochemically reduced GO (45-min reduction).

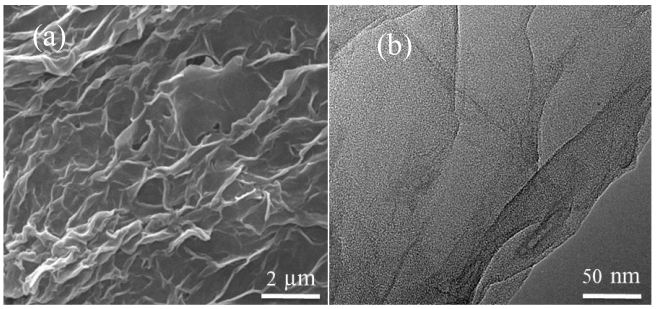

FIGURE 5. (a) SEM and (b) TEM image of the photochemically reduced GO with a UV exposure time of 45 minutes.

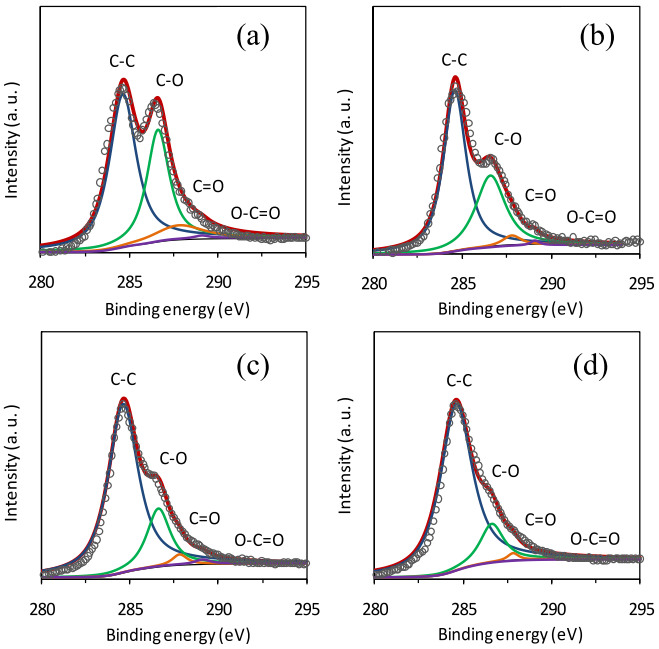

FIGURE 6. C1s XPS spectra of GO by photochemical reduction after a reaction time of (a) 0 min, (b) 15 min, (c) 30 min, and (d) 45 min. Circles: experiment data points, red curve: theory fitting; other color curves are theory for individual chemical groups: black for C-C, green for C-O, orange for C=O and blue for O-C=O.

microscopy (Fig. 5b) showing folded and wrinkled rGO sheets in a large area, and three to five layers at the edge of rGO sheets.

XPS was performed to quantify GO reduction and recorded the gradual reduction evolution of carbon atoms during photochemical reduction (Fig. 6 a-d). Four types of carbon with different chemical states were identified for GO, including the characteristic peaks at 284.6 eV (graphite, C-C), 286.6 eV (C-O), 287.8 eV (C = O) and 289.1 eV (O-C = O) respectively. For rGO with 45-min light exposure, the content of -C-O, -C = O, O = C-O groups decreased 59.1 %, 86.7 %, and 91.3 %, and the content of C-C and C = C groups increased 54.0%, demonstrating the effective photochemical reduction of GO. The time-course reductions of oxygenated functional groups were summarized in Fig. 7.

FTIR and Raman spectroscopy were used to characterize the composition. The FTIR spectra (Fig. 8a) showed the bands of oxygen-containing groups, such as 3415 cm^{-1} for O-H, 1730 cm^{-1} for C = O, 1417 cm^{-1} for epoxy C-O, 1055 cm^{-1} for alkoxy C-O. In particular, the peak located at 1625 cm^{-1} was assigned to the contribution from the skeletal vibrations of the graphitic domain. After 45-min UV irradiation, the carboxylic acid vibration band (1730 cm^{-1}) almost disappeared, and only a weak signal of O-H (3415 cm^{-1}) could be detected, indicating the existence of adsorbed water molecules. Raman spectroscopy is able to identify the presence of defects on the graphene carbon network by measuring the D (defects in the curved graphene sheet, and staging disorder, 1346 cm^{-1}) and G

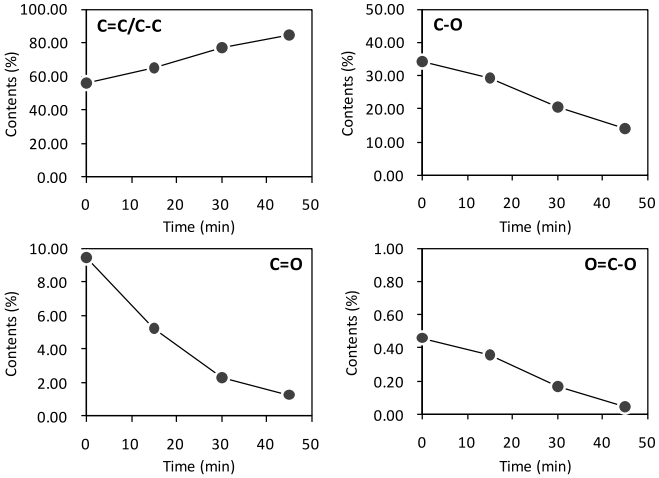

FIGURE 7. Contents of the functional groups with respect to the reaction time during the photochemical reduction of GO by Irgacure-907. The data were derived from the C1s XPS spectra shown in Fig. 6.

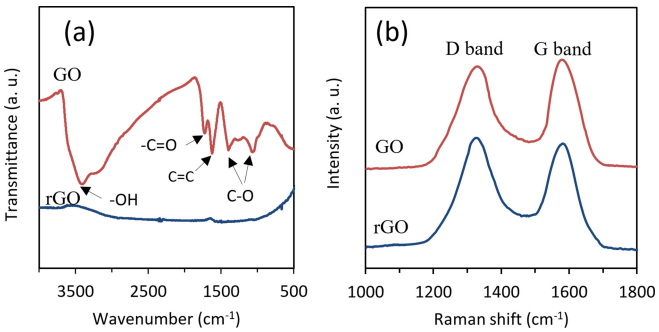

FIGURE 8. (a) FTIR and (b) Raman spectra of GO dispersion before and after photochemical reduction (UV exposure for 45 min).

(graphitic, sp^2 bonded carbon, 1600 cm^{-1}) bands. With the reduction, the ratio of the peak intensities of D/G increased to 1.06 for rGO compared with 0.92 for GO prior to the photochemical reduction (Fig. 8b), which was usually observed in Raman spectra of hydrazine reduced GO because of the size of sp^2 domain decreased as the rGO sheet was broken into fragments during photochemical reduction.

All the results above show that the oxygenated groups were successfully removed from the original GO solution photochemically. Still, electrical conductivity is counted most importantly, deciding the competency in inkjet printing. To accurately measure the improvement in conductivity compared with original GO powders, I followed a power compression protocol [35] and a four-point probe (ST2253,Suzhou Jingge Electronic Co., Ltd., China.) method to measure the electrical conductivity of the compressed disk.The conductivity of individual flakes is expected to be significantly lower since there were pockets of air between the particles in the compressed disk. At room temperature, the rGO from photochemical reduction had a conductivity of 3×10^3 S/m, which improved by 6 orders from the original GO. The conductivity of the rGO product is comparable to graphene composite of high electric conductivity [22], [36], also it is 1-2 orders higher than infrared (IR) lamp-reduced graphene [24]. The conductivity of the photochemically reduced rGO was compared with the commercially available graphene (Suzhou Tanfeng Graphene Technology Co., Ltd., China.). Following the same four touchpoints protocol, the acquired few-layer graphene showed a conductivity of 200 S/m, which is one-fold lower than the rGO from photochemical reduction.

IV. CONCLUSION

In summary, a photochemical reduction based technology to produce rGO nanosheets from GO powder were developed. The carbonyl and hydroxyl groups presented in GO have hydrophilic nature and can be uniformly mixed with the photoinitiator Irgacure-907. When exposing to UV light, Irgacure-907 in the aqueous mixture generates the strong reducing α-aminoalkyl (α-A*) radicals which serve as an electron donor and processes stronger reducing powers to remove oxygen-containing functional groups of GO. Quantitative GO reduction by UV light dosage was demonstrated, either by adjusting illumination time or intensity. Spectroscopic and imaging techniques showed GO was successfully reduced to rGO. The conductivity of the compressed disc also showed high conductivity, consistent with graphene nanosheet of high purity.

The one-step synthesis of graphene involving composite has a good potential to be made into nanomaterial and UV curable resin for applications in stereolithography apparatus (SLA) and computed axial lithography (CAL). Working with other frontier technologies, the photochemically produced rGO is an ideal candidate for designing personalized micro and nanodevices. Examples of such devices include but not limited to electronic devices, solar energy storage and conversion, fuel cell electrodes and catalyst carriers.

ACKNOWLEDGMENT

The author would like to thank Prof. Yulong Zhao at Xi'an Jiaotong University for his generous support and insightful suggestions for this work.

REFERENCES

[1] H. K. Chae *et al.*, "A route to high surface area, porosity and inclusion of large molecules in crystals," *Nature*, vol. 427, no. 6974, pp. 523–527, Feb. 2004. doi: 10.1038/nature02311.

[2] A. A. Balandin *et al.*, "Superior thermal conductivity of single-layer graphene," *Nano Lett.*, vol. 8, no. 3, pp. 902–907, Mar. 2008. doi: 10.1021/nl0731872.

[3] C. Lee, X. Wei, J. W. Kysar, and J. Hone, "Measurement of the elastic properties and intrinsic strength of monolayer graphene," *Science*, vol. 321, no. 5887, pp. 385–388, Jul. 2008. doi: 10.1126/science.1157996.

[4] X. Li, Y. Zhu, W. Cai, M. Borysiak, and B. Han, "Transfer of large-area graphene films for high-performance transparent conductive electrodes," *Nano Lett.*, vol. 9, no. 12, pp. 4359–4363, Dec. 2009. doi: 10.1021/nl902623y.

[5] K. S. Novoselov *et al.*, "Electric field effect in atomically thin carbon films," *Science*, vol. 306, no. 5696, pp. 666–669, Oct. 2004. doi: 10.1126/science.1102896.

[6] Z. Sun *et al.*, "ZnO nanowire-reduced graphene oxide hybrid based portable NH_3 gas sensing electron device," *IEEE Electron Device Lett.*, vol. 36, no. 12, pp. 1376–1379, Dec. 2015. doi: 10.1109/LED.2015.2496177.

[7] J.-C. Chou, C.-H. Huang, Y.-H. Liao, S.-W. Chuang, L.-H. Tai, and Y.-H. Nien, "Effect of different graphene oxide contents on dye-sensitized solar cells," *IEEE J. Photovolt.*, vol. 5, no. 4, pp. 1106–1112, Jul. 2015. doi: 10.1109/JPHOTOV.2015.2419137.

[8] M. Sanaeepour, A. Abedi, and M. J. Sharifi, "Performance analysis of nanoscale single layer graphene pressure sensors," *IEEE Trans. Electron Devices*, vol. 64, no. 3, pp. 1300–1304, Mar. 2017. doi: 10.1109/TED.2017.2656944.

[9] H. Sun, K. Xu, G. Lu, H. Lv, and Z. Liu, "Graphene-supported silver nanoparticles for pH-neutral electrocatalytic oxygen reduction," *IEEE Trans. Nanotechnol.*, vol. 13, no. 4, pp. 789–794, Jul. 2014. doi: 10.1109/TNANO.2014.2322091.

[10] J. Kim *et al.*, "Bioactive effects of graphene oxide cell culture substratum on structure and function of human adipose-derived stem cells," *J. Biomed. Mater. Res. A*, vol. 101, no. 12, pp. 3520–3530, Dec. 2013. doi: 10.1002/jbm.a.34659.

[11] A. S. T. Smith *et al.*, "Micro- and nano-patterned conductive graphene–PEG hybrid scaffolds for cardiac tissue engineering," *Chem. Commun.*, vol. 53, no. 53, pp. 7412–7415, Jun. 2017. doi: 10.1039/c7cc01988b.

[12] Q. Zhang, F. Zhang, S. P. Medarametla, H. Li, C. Zhou, and D. Lin, "3D printing of graphene aerogels," *Small*, vol. 12, no. 13, pp. 1702–1708, Apr. 2016. doi: 10.1002/smll.201503524.

[13] J. R. McGhee, M. Sinclair, D. J. Southee, and K. G. U. Wijayantha, "Strain sensing characteristics of 3D-printed conductive plastics," *Electron Lett.*, vol. 54, no. 9, pp. 570–572, May 2018. doi: 10.1049/el.2018.0363.

[14] J. H. Kim, W. S. Chang, D. Kim, J. R. Yang, J. T. Han, and G. W. Lee, "3D printing of reduced graphene oxide nanowires," *Adv. Mater.*, vol. 27, no. 1, pp. 157–161, Jan. 2015. doi: 10.1002/adma.201404380.

[15] D. Kokkinis, M. Schaffner, and A. R. Studart, "Multimaterial magnetically assisted 3D printing of composite materials," *Nat. Commun.*, vol. 6, no. 8643, pp. 1–10, Oct. 2015. doi: 10.1038/ncomms9643.

[16] X. Lu, M. Yu, H. Huang, and R. S. Ruoff, "Tailoring graphite with the goal of achieving single sheets," *Nanotechnology*, vol. 10, no. 3, p. 269, Sep. 1999. doi: 10.1088/0957-4484/10/3/308.

[17] K. K. Nagothu, A. Mishra, A. Meersha, and M. Shrivastava, "On the ESD behavior of large-area CVD graphene transistors: Physical insights and technology implications," *IEEE Trans. Electron Devices*, vol. 66, no. 1, pp. 743–751, Jan. 2019. doi: 10.1109/TED.2018.2877693.

[18] S. Park and R. S. Ruoff, "Chemical methods for the production of graphenes," *Nat. Nanotechnol.*, vol. 4, no. 4, pp. 217–224, Apr. 2009. doi: 10.1038/nnano.2009.58.

[19] M. M. Stylianakis, M. Sygletou, K. Savva, G. Kakavelakis, E. Kymakis, and E. Stratakis, "Photochemical synthesis of solution-processable graphene derivatives with tunable bandgaps for organic solar cells," *Adv. Opt. Mater.*, vol. 3, no. 5, pp. 658–666, Dec. 2015. doi: 10.1002/adom.201400450.

[20] G. Eda, G. Fanchini, and M. Chhowalla, "Large-area ultrathin films of reduced graphene oxide as a transparent and flexible electronic material," *Nat. Nanotechnol*, vol. 3, no. 5, pp. 270–274, May 2008. doi: 10.1038/nnano.2008.83.

[21] C. K. Chua and M. Pumera, "Reduction of graphene oxide with substituted borohydrides," *J. Mater. Chem. A*, vol. 1, no. 5, pp. 1892–1898, Jan. 2013. doi: 10.1039/C2TA00665K.

[22] J. Li, F. Ye, S. Vaziri, M. Muhammed, M. C. Lemme, and M. Östling, "Efficient inkjet printing of graphene," *Adv. Mater.*, vol. 25, no. 29, pp. 3985–3992, Aug. 2013. doi: 10.1002/adma.201300361.

[23] K.-Y. Shin, J.-Y. Hong, and J. Jang, "Micropatterning of graphene sheets by inkjet printing and its wideband dipole-antenna application," *Adv. Mater.*, vol. 23, no. 18, pp. 2113–2118, May 2011. doi: 10.1002/adma.201100345.

[24] D. Kong, L. T. Le, Y. Li, J. I. Zunino, and W. Lee, "Temperature-dependent electrical properties of graphene inkjet-printed on flexible materials," *Langmuir*, vol. 28, no. 37, pp. 13467–13472. Sep. 2012. doi: 10.1021/la301775d.

[25] Y. Tu, T. Ichii, T. Utsunomiya, and H. Sugimura, "Vacuum-ultraviolet photoreduction of graphene oxide: Electrical conductivity of entirely reduced single sheets and reduced micro line patterns," *Appl. Phys. Lett.*, vol. 106, no. 13, Apr. 2015, Art. no. 133105. doi: 10.1063/1.4916813.

[26] J. D. Mangadlao, P. Cao, D. Choi, and R. C. Advincula, "Photoreduction of graphene oxide and photochemical synthesis of graphene–metal nanoparticle hybrids by ketyl radicals," *ACS Appl. Mater. Interfaces*, vol. 9, no. 29, pp. 24887–24898, Jul. 2017. doi: 10.1021/acsami.7b06275.

[27] Y. H. Ding, P. Zhang, Q. Zhuo, H. M. Ren, Z. M. Yang, and Y. Jiang, "A green approach to the synthesis of reduced graphene oxide nanosheets under UV irradiation," *Nanotechnology*, vol. 22, no. 21, pp. 215601–215606, Mar. 2011. doi: 10.1088/0957-4484/22/21/215601.

[28] C. Karin, F. Tim, C. Xianjue, L. Shiyang, and Z. Chuan, "One-step photochemical synthesis of transition metal–graphene hybrid for electrocatalysis," *ACS Sustain. Chem. Eng.*, vol. 7, no. 4, pp. 4112–4118, Jan. 2019. doi: 10.1021/acssuschemeng.8b05607.

[29] T.-L. Wee *et al.*, "Photochemical synthesis of a water oxidation catalyst based on cobalt nanostructures," *J. Amer. Chem. Soc.*, vol. 133, no. 42, pp. 16742–16745, Oct. 2011. doi: 10.1021/ja206280g.

[30] N. I. Kovtyukhova *et al.*, "Layer-by-layer assembly of ultrathin composite films from micron-sized graphite oxide sheets and polycations," *Chem. Mater.*, vol. 11, no. 3, pp. 771–778, Jan. 1999. doi: 10.1021/cm981085u.

[31] H. A. Becerril, J. Mao, Z. Liu, R. M. Stoltenberg, Z. Bao, and Y. Chen, "Evaluation of solution-processed reduced graphene oxide films as transparent conductors," *ACS Nano*, vol. 2, no. 3, pp. 463–470, Mar. 2008. doi: 10.1021/nn700375n.

[32] Y. Xu, H. Bei, G. Lu, C. Li, and G. Shi, "Flexible graphene films via the filtration of water-soluble noncovalent functionalized graphene sheets," *J. Amer. Chem. Soc.*, vol. 130, no. 18, pp. 5856–5857, May 2008. doi: 10.1021/ja800745y.

[33] C. J. Shearer, A. D. Slattery, A. J. Stapleton, J. G. Shapter, and C. T. Gibson, "Accurate thickness measurement of graphene," *Nanotechnology*, vol. 27, no. 12, Mar. 2016, Art. no. 125704. doi: 10.1088/0957-4484/27/12/125704.

[34] V. Georgakilas *et al.*, "Noncovalent functionalization of graphene and graphene oxide for energy materials, biosensing, catalytic, and biomedical applications," *Chem. Rev.*, vol. 116, no. 9, pp. 5464–5519, May 2016. doi: 10.1021/acs.chemrev.5b00620.

[35] B. Marinho, M. Ghislandi, E. Tkalya, C. E. Koning, and G. de With, "Electrical conductivity of compacts of graphene, multi-wall carbon nanotubes, carbon black, and graphite powder," *Powder Technol.*, vol. 221, pp. 351–358, May 2012. doi: 10.1016/j.powtec.2012.01.024.

[36] G. Kaur *et al.*, "Graphene/polyurethane composites: Fabrication and evaluation of electrical conductivity, mechanical properties and cell viability," *RSC Adv.*, vol. 5, no. 120, pp. 37553–37567, Nov. 2015. doi: 10.1039/C5RA20214K.

HONGLIANG SUN (M'13) received the B.S. degree in automation and the M.S. degree in control theory and control engineering from the Kunming University of Science and Technology, China, in 2004 and 2009, respectively. He is currently pursuing the Ph.D. degree with Xi'an Jiaotong University. In 2013, he became an Associate Professor of Yunnan Open University. He was a Visiting Scholar with the College of Chemistry and Molecular Engineering, Peking University from 2013 to 2015, and the Department of Chemistry, University of Colorado at Boulder from 2016 to 2018. He is an Adjunct Faculty with Yunnan University. His broad interests include MEMS, bionics, nanodevices, and 3-D printing.